Current Research in Microbial Sciences 2 (2021) 100021

Contents lists available at ScienceDirect

Current Research in Microbial Sciences

journal homepage: www.elsevier.com/locate/crmicr

Topography effect on Aspergillus flavus occurrence and aflatoxin B1 contamination associated with peanut

Yanpo Yao[a,b,c,d,e], Suyan Gao[a,b,c,d,e], Xiaoxia Ding[a,b,c,d,e], Qi Zhang[a,b,c,d,e,*], Peiwu Li[a,b,c,d,e,*]

[a] Oil Crops Research Institute, Chinese Academy of Agricultural Sciences, Wuhan 430062, China
[b] Key Laboratory of Biology and Genetic Improvement of Oil Crops, Ministry of Agriculture, Wuhan 430062, China
[c] Key Laboratory of Detection for Mycotoxins, Ministry of Agriculture, Wuhan 430062, China
[d] Laboratory of Risk Assessment for Oilseeds Products, Wuhan, Ministry of Agriculture, Wuhan 430062, China
[e] Quality Inspection and Test Center for Oilseeds Products, Ministry of Agriculture, Wuhan 430062, China

ARTICLE INFO

Keywords:
Topography
Aflatoxin contamination
Microbiota
Metatranscriptome
Metabolomics
Environmental factors

ABSTRACT

Aflatoxin B_1 is a strong carcinogenic and toxic fungal toxin produced by Aspergillus flavus and other Aspergillus species, and can seriously threaten the health of consumers and the safety and quality of agricultural products. Aspergillus in agricultural products are closely related to topography and symbiotic microbes. It is not fully clear that how topography affects the assembly process of A. flavus and symbiotic fungi on plant. In this study, we analyzed the structure and assembly process of fungi on the peanut. We also performed the metatranscriptome analysis, identified the functional genes and metabolic pathways enriched in both A. flavus and its symbiotic fungi. In our experiment, terrain and soil properties could significantly affect the gene expression of microbiome, A. flavus abundance and infection ability to peanuts. Meanwhile, the Permanova correlation analysis revealed that differentially expressed genes were strongly correlated with the soil physicochemical factors. Furthermore, metabolomic analysis identified the main metabolites associated with A. flavus and aflatoxin B_1, the results proved that the terrain significantly affected the microorganisms associated with peanut pods to produce a variety of metabolites. In conclusion, our results indicate that topography can significantly influence the assembly process of A. flavus and microorganisms, the activation of functional genes and metabolic pathways, the enrichment of aflatoxin-producing fungi.

1. Introduction

Peanuts is one of the world's five major oil crops, widely planted in developing countries such as Asia, Africa, South America and some developed countries such as the United States (Archer, 2016). Peanut plays an important role in the world's agricultural production and trade (Santos, 2000). In 2016, the world's total output was about 41,000 kt and the planting area was about 24,000 khm^2, ranking third only to soybean and rapeseed among oil crops. China is the main producer of peanut in the world, with an annual planting area of 5000 khm^2, accounting for 20% of the world's total planting area, ranking second; an output of 17,000 kt, accounting for 45% of the world's total production, ranking first (http: //faostat.fao.org). China occupies a leading position in the international peanut export trade and is the world's largest exporter of peanut, with an average annual export volume of 700 kt, accounting for about 40% of the world's peanut product trade volume (http://data.stats. gov. cn/easyquery.htm?cn=C01).

The quality and safety of peanut products can be affected by many factors, including those such as aflatoxin B_1 contamination, temperature, humidity, physical and chemical properties of soil (Nataraj et al., 2016; Han et al., 2019; Dong et al., 2018; Zhao et al., 2019; Xia et al., 2019; Subhashini., 2016). With the rapid increase in peanut production and consumption, aflatoxin B_1 contamination is raising concern. The Yangtze River zone, Jiangxi Province, China, is the major peanut-producing region of the country and has a subtropical climate with high temperatures and high relative humidity, which is the favorable environmental condition for A. flavus growth and aflatoxins B_1 production on peanuts. Aflatoxin is a secondary metabolite of A. flavus (Link) and A. parasiticus (Speare), belongs to the strongest carcinogenic chemical in nature (Bankole et al., 2004; Williams et al., 2004; Barros et al., 2003).

* Corresponding author at: Oil Crops Research Institute, Chinese Academy of Agricultural Sciences, Wuhan 430062, China.
E-mail address: peiwuli@oilcrops.cn (Q. Zhang).

https://doi.org/10.1016/j.crmicr.2021.100021
Received 18 November 2020; Received in revised form 1 February 2021; Accepted 3 February 2021

Peanut is highly susceptible to Aspergillus infection and the consequent aflatoxin B_1 contamination (Passone et al., 2010; Santos et al., 2001; CEC, 2010). Aflatoxin B_1 contamination seriously hinders the sustainable development of the peanut industry, particularly in southern China. Environmental factors, such as water activity and temperature, influence A. flavus growth and aflatoxin production (Giorni et al., 2009). The studies suggest that endophytic A. flavus is derived from local soil but not from the seed source, and some fungi show inhibitory effects against A. flavus. Therefore, soil properties and the symbiotic microbiome are critical for aflatoxin B_1 production and food safety in peanuts. Thus, it is important to explore the microbiome composition of the peanut rhizosphere and their impacts on toxin production. The study of the peanut rhizosphere microbiome is highly challenging because most microorganisms cannot be isolated and cultured alone. However, the use of next-generation sequencing provides a new technology to study the microbiome of the peanut rhizosphere (Fitzpatrick et al., 2018; Chen et al., 2018).

In addition, this approach enables us to screen symbiotic microbes associated with the stress tolerance of host plants (Chen et al., 2018). Recent studies have helped to elucidate the correlation between symbiotic microbes and environmental factors, diseases and host plants (Fitzpatrick et al., 2018; Chen et al., 2018; Devin et al., 2016; Dan et al., 2017; Tas et al., 2018). Research has shown that root symbiotic microorganism populations influence fungal composition (Chen et al., 2018), but studies concerning microbiota and A. flavus and aflatoxin B_1 remain limited. Our previous research showed that cultivating regions significantly influence A. flavus abundance and aflatoxin B_1 production in peanuts. However, the role of topography has not been elucidated to date, which hinders the preventive management of aflatoxin.

In this study, we examined the microbiota on and around peanut pods from experimental plots at various terrains. The parameters including microbiota composition, function, metabolic pathways, and metabolites were analyzed to evaluate their effects on A. flavus abundance and aflatoxin production. We further analyzed the association between the physical and chemical properties of soil in different terrains and microbiota, their functions and their relationship with A. flavus. These results will promote the development of aflatoxin contamination prediction and control systems.

2. Materials and methods

2.1. Sample collection

Based on our previous research, experimental plots in Zhangshu, Jiangxi (27.9346°N, 115.3114°E) were selected to collect the samples because they suffer the most serious aflatoxin contamination problem and represent the typical topography of the peanut planting areas in southern China (Ding et al., 2015a,b). The investigation area included five experimental plots at three different slope positions, all of plots are faced to the sun. Fifty samples, including soil around and on the peanut pod, were collected from experimental plots A and B (soil sample IDs are the following: around-the-pod samples from plot A: A1T, uphill position (75 m above sea level), 8 samples; A2T, medium position (70 m above sea level), 8 samples; A3T, downhill position (65 m above sea level), 8 samples; around-the-pod samples from plot B: B1T, uphill position (73 m above sea level), 8 samples; B2T, medium position (68 m above sea level), 8 samples. On-the-pod samples: AK, 7 samples from plot A; BK, 3 samples from plot B. We respectively evaluated the soil physical and chemical properties between plot A and plot B on terrain, in addition to water activity, no significant differences in other physical and chemical properties of soil (Supplementary Table 15) . The around-the-pod soil samples compartment was composed of ~1 mm of soil tightly adhering to the pod surface that is not easily shaken from the pod. The on-the-pod sample compartment microbiome was derived from the suite of microbes on the pod surface that cannot be removed by washing in buffer but is removed by sonication. Control soil samples collected from the same experimental plot were processed in parallel, the control was 20 cm away from the root and corresponding to the peanut plant. The samples with the highest and lowest abundances of Aspergillus flavus were selected for ITS amplicon analysis. Metatranscriptome analysis of the corresponding soil samples on the peanut pods were also performed. Mature peanut plants with entire roots were harvested. Roots were separated from the stems, and pods were collected. In parallel, normal and ultrasonic cleaning were combined to separate the microbiome in the peanut pods and on the peanut pods. Peanut pods were socked with sterile filter paper. Clean peanuts and 20 g soil were snap-frozen with liquid nitrogen and stored at −80 °C until use. Another 80 g of soil was subjected to analysis of the physical and chemical properties.

2.2. DNA sequencing and analysis

Total DNA from samples was extracted using the E.Z.N.A. Soil DNA Kit (Omega Bio-tek, Norcross, GA, USA). PCR-based library construction targeting the internal transcribed spacer (ITS) was performed and then sequenced on an Illumina HiSeq 2500 instrument (Illumina, SanDiego, CA, USA) using a 250 bp paired-end (PE) sequencing method. Raw reads were filtered with an in-house pipeline and assembled into consensus sequences by FLASH (Fast Length Adjustment of Short reads, v1.2.11) (Bokulich et al., 2013) based on the overlapping of the two paired-end reads.

We used Uparse software (Uparse v7.0.1001, http://drive5.com/uparse/) to perform 97% and 95% identity clustering on all the effective tags of all samples to form OTUs (Operational Taxonomic Units) ; we then selected the representative OUTs sequences and used the assign-taxonomy script (http://qiime.org/scripts/ assign-taxono-my.html) in QIIME together with the Unite (ITS, http://unite.ut.ee/index.php) database for species annotation (Edgar et al., 2018; Quast et al., 2013). Weighted and unweighted UniFrac distance analysis was performed based on the abundance of OTUs and phylogenetic tree. Principal coordinate analysis (PCOA) was conducted based on the UniFrac distance by customized R (version 3.3.3) scripts. Alpha and beta diversity and rarefaction curves were analyzed based on the relative abundance table of OTUs (Koljalg et al., 2013; Chen et al., 2012).

2.3. Transcriptome analysis

Eukaryotic mRNA was enriched with magnetic Oligo-dT beads from total RNA. mRNA was sheared in fragmentation buffer. Random hexamers were added to synthesize the reverse complementary DNA (cDNA). A mixture of buffer, dNTPs, RNase H and DNA polymerase I was added to synthesize the second strand of cDNA, which was then purified with a QiaQuick PCR kit and eluted with EB buffer. DNA fragment ends were ligated with adapters after adenylation and then subjected to agarose electrophoresis for size selection. After PCR amplification, the constructed libraries were sequenced with Illumina HiSeq 2500 (Love et al., 2014).

Reads were trimmed to guarantee the quality of raw data based on the in-house scripts. Reads with N content over 10%, adaptor contamination and low quality were removed. Trinity (http://trinityrnaseq.sourceforge.net/) was applied to reconstruct the full-length transcripts, which were further processed by Tgicl to exclude redundant and chimeric assemblies and homologous transcript clusters. The resulting nonredundant unigenes were aligned to reference databases, including NR, Swiss-Prot, KEGG and COG, by blasting (e-value < 0.00001) to obtain annotation of gene and species information. Expression levels of unigenes were calculated by RPKM (reads per kb per million reads). Finally, fold change of gene expression comparing various samples was calculated by FPKM value. A gene with an FDR less than 0.001 and

a fold change above 2 was defined as a significantly differentially expressed gene (Love et al., 2014).

2.4. Metabolomics analysis

In a 5 mL EP tube, 1 g ± 1 mg of sample, 1 mL of extraction liquid (methanol:dH_2O 3:1, v/v), 1 mL of ethyl acetate, and 5 μL of L-2-chlorophenylalanine (1 mg/mL stock in dH_2O) were added, vortexed for 30 s, and homogenized in a ball mill for 4 min at 45 Hz followed by 5 min of sonication (incubated in ice water). The homogenization process was repeated 6 times. Samples were centrifuged for 15 min at 10,000 rpm at 4 ˚C. One milliliter of supernatant was transferred into a fresh 1.5 mL EP tube. Samples were dried completely in a vacuum concentrator without heating. Next, 20 μL of methoxy amination hydrochloride (20 mg/mL in pyridine) was added and incubated for 30 min at 80 ˚C. Then, 30 μL of the BSTFA regent (1% TMCS, v/v) was added to the sample aliquots and incubated for 1.5 h at 70 ˚C. All samples were analyzed by gas chromatography coupled with a Pegasus BT time-of-flight mass spectrometer (LECO, Pegasus BT, USA).

GC-TOF-MS analysis was performed using an Agilent 7890 gas chromatograph system coupled with a Pegasus HT time-of-flight mass spectrometer. The system utilized a DB-5MS capillary column coated with 5% diphenyl cross-linked with 95% dimethylpolysiloxane (30 m × 250 μm inner diameter, 0.25 μm film thickness; J&W Scientific, Folsom, CA, USA). A 1 μL aliquot of the analyte was injected in splitless mode. Helium was used as the carrier gas, the front inlet purge flow was 3 mL min^{-1}, and the gas flow rate through the column was 1 mL min^{-1}. The initial temperature was kept at 50 ˚C for 1min, then raised to 310 ˚C at a rate of 10 ˚C min^{-1}, then kept for 8 min at 310 ˚C. The injection, transfer line, and ion source temperatures were 280, 280, and 250 ˚C, respectively. The energy was −70 eV in electron impact mode. The mass spectrometry data were acquired in full-scan mode with the m/z range of 50–500 at a rate of 12.5 spectra per second after a solvent delay of 6.17 min.

2.5. Analysis of the soil physical-chemical properties

The amounts of nutrient elements (effective K, Cu, Zn, Fe, Mn) in the soil were measured by a plasma emission spectrometer (PE company, Optima 7300 V). Two grams of air-dried soil sample was transferred to a 100 mL digestion tube, in which 15 mL of HCL and 5 mL of HNO_3 (ρ = 1.42 g/mL) were added to digest the soil with shaking for 30 min. The digestion solution was filtered, scaled up to 100 mL, and measured with the ICP spectrometer. Standard solution and 5% HNO_3 were mixed in a 25-mL volumetric flask for a standard curve. The absorbance of different concentrations of the standard solution was measured to generate the standard curve with 5% HNO_3 solution serving as a blank. The soil sample solution was then measured to calculate the amounts of nutrient elements in the soil.

Organic substances in the soil were determined by the potassium dichromate method. Air-dried soil (0.05–0.5 g, 100 mesh) was transferred into a 150 mL Erlenmeyer flask. A small amount of solid silver sulfate, 5.0 mL of 0.8 mol/L potassium dichromate, and 5 mL of H_2SO_4 were added, in turn. The mixture was well shaken and placed on a 220 ˚C hot plate with a cold air pipe inserted into the flask neck. The flask was heated for 8 min until the liquid in the air pipe cooling tube raised and began to fall. The flask was then removed from the plate. The air-cooling pipe was rinsed with dH_2O several times to a final volume of 60–70 mL. A standard solution of ferrous sulfate was used for titration until the color of the solution changed from orange to cyan and then brownish red. Experiments with silica powder as a replacement for the soil sample were conducted once or twice as a blank test (Zhang et al., 2019).

The total nitrogen in the soil was dissolved with concentrated sulfuric acid by heating in a 300 W electric furnace. The total phosphorus was alkali melted with sodium hydroxide at 720 ˚C. The digestion solution was analyzed by Kjeldahl nitrogen, molybdenum blue colorimetry, and flame photometry. In detail, (0.3 ± 0.01) g of air-dried soil (100-mesh) was well mixed with 4 mL of concentrated sulfuric acid with shaking. Hydrofluoric acid (1.2 mL) was added three times with shaking. Then, 0.3 mL of perchloric acid was added. The digestion tube was tightly capped and heated at 195 ˚C for 4 h in an automatic digestion apparatus. Later, after the solution was completely cooled, with the cap open, the tube was heated at 120 ˚C for 30 min on a hot plate to remove hydrofluoric acid. The solution was cooled and diluted to 100 mL in a volumetric flask for further tests.

2.6. Analysis of Aflatoxin B_1

2.6.1. Sample pretreatment

Accurate to take 2 g (0. 001 g) peanut samples in a 50 mL centrifuge tube, 10 mL of 80% acetonitrile-water solution was added, swirled and mixed for 30 s, soaked for 30 min, oscillated for 1 h and then sonicated under 500 W power Extract for 30 min, centrifuged at 10,000 r/min for 10 min, the supernatant was gathered and purified on MyCOsepTM226 multi-function column, 5 mL of the purified solution was dried in nitrogen at 50 ˚C, dissolved in 1.0 mL of 50% methanol, and then eddy mixed for 30 s. The solution was filtered with 0.22 μm microporous filter membrane into the injection flask for UPLC-MS-MS detection (Zhang et al., 2015; Ding et al., 2015a,b; Wu et al., 2016).

2.6.2. Solution preparation

2.6.2.1. Solvent mixed standard working solution. The AFB_1 standard was mixed with 50% methanol solution to prepare the solvent mixed standard working solution with mass concentration of 0.1, 0.2, 1, 5, 10, 20 μg/L, configure when used.

2.6.2.2. Matrix mixed standard working solution. Peanut sample without aflatoxin was pretreated to obtain a blank sample extract. The AFB_1 standard was mixed with blank sample extract to prepare the matrix mixed standard working solution with mass concentration of 0.1, 0.2, 1, 5, 10, 20 μg/L, configure when used.

2.6.2.3. Mass spectrometry conditions optimization working solution. The AFB_1 standard was mixed with 50% methanol solution to prepare the AFB_1 solution with mass concentration of 50 μg/L for the optimization of mass spectrum conditions.

2.6.3. Chromatographic conditions

Chromatographic column: Kinetex SB - C18 (100 mm × 2.1 mm, 1.7 μm); Mobile phase: Phase A is 0.1% formic acid solution, and phase B is methanol. The gradient elution procedure is as follows: 0-8 min, 30–100% B; 8–13 min, 100% B; 13.1–20 min, 30% B; Column temperature: 40 ˚C; Injection volume: 3 μL.

2.6.4. Mass spectrometry conditions

Scaning mode: positive ion scaning; monitoring mode; multi-reactive ion monitoring MRM; ion source temperature: 550 ˚C; ionization voltage: 5500 V; curtain air pressure: 206.9 kPa; atomizing gas pressure: 379.2 kPa; auxiliary gas pressure: 379.2 kPa.

2.7. Statistical analysis

Beta diversity analysis was used to evaluate differences of samples in species complexity. Based on ITS abundance, Bray_curtis, unweighted-uniFrac, and weighted-uniFrac algorithms were calculated by QIIME software and PCoA (principle coordination analysis) was used to assess the variation in the composition of microbial communities between paired samples. PERMANOVA (permutational multivariate analysis of variance) was used to calculate the difference and significance between samples (vegan package in R). Alpha diversity (based on the Chao1 and

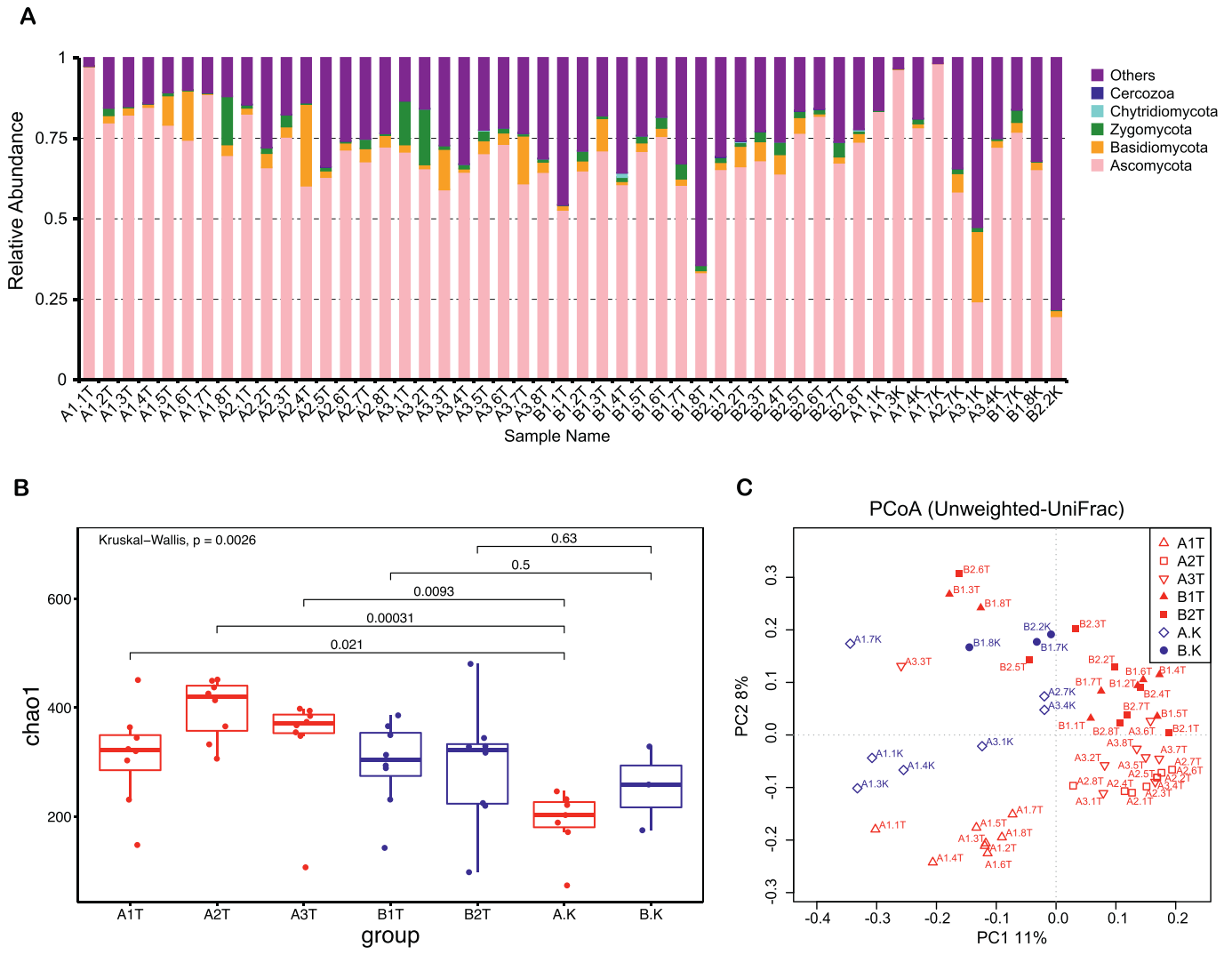

Fig. 1. The population structure of the soil fungi around and on the surface of pod under different topography. (a) The relative abundance of fungi composition in the 50 samples at the phylum level. Soil sample ID are as follows: around-the-pod samples from experimental plots A: A1T, 8 samples; A2T, 8 samples; A3T, 8 samples; around-the-pod samples from experimental plots B: B1T, 8 samples; B2T, 8 samples. On-the-pod samples: A.K, 7 samples from experimental plot A; B.K, 3 samples from experimental plot B. (b) Alpha diversity of 50 samples from 7 groups in accordance with chao1 index and wilcox.test's *p*-value between 2 sample groups. (c) The PCoA plot of 50 samples from 7 groups.

Shannon index) between groups was calculated by the Wilcoxon rank-sum test. Variance of gene expression and metabolites were calculated by the Kruskal–Wallis test. The Spearman coefficient was used to calculate the correlation between microorganisms, gene transcription and metabolites. (Buttigieg and Ramette, 2014).

3. Results and discussion

3.1. Fungal diversity on peanut pods and effects of topography

The enrichment of fungi in each sample was examined by ITS sequencing. A total of 2,262,088 fungal ITS tags with high quality were obtained with an average of 45,242 per sample (Supplementary Table 1). A total of 2,334 OTUs were obtained after clustering analysis with an average of 302 per sample (Supplementary Table 2).

There were no significant differences at the phylum level. At the genus level, Lodderomyces and (Basidiobolus were only detected on the peanut pod, while Arthrobotrys, Periconia, and Purococillium were found only in the soil around the pod. OTUs in more than 90% of the 10 samples collected around or on the peanut pod were considered core OTUs. According to these criteria, 35 and 31 core OTUs were obtained from around-the-pod and on-the-pod samples, respectively (Supplementary Table 4). Ascomycota accounted for 69.43% of the total enriched fungi, which was the most abundant fungal population related to peanuts in either around-the-pod or on-the-pod soil samples. Basidiomycota (4.32%), Zygomycota (2.30%) and Chytridiomycota (0.05%) were the top 3 species following Ascomycota. Mortierella (2.28%), Aspergillus (2.34%), and Fusarium (1.71%) were the most abundant fungi at the genus level. Next, 10 on-the-pod samples and their corresponding around-the-pod soil samples were subjected to paired tests, and 6 fungal genera showed a significant difference in abundance (Wilcoxon test, *P*-value < 0.05, Supplementary Table 3, Fig.1A).

Alpha diversity between on-the-pod samples and around-the-pod soil was compared. As shown in Fig. 1B, the higher Chao1 of around-the-pod soil versus on-the-pod samples was consistent in plot A with uphill position, medium position and downhill position. However, this phenomenon of the B plot is not as obvious as that of the A plot, indicating that geographic factors also contribute to species diversity (Fig. 1A–C).

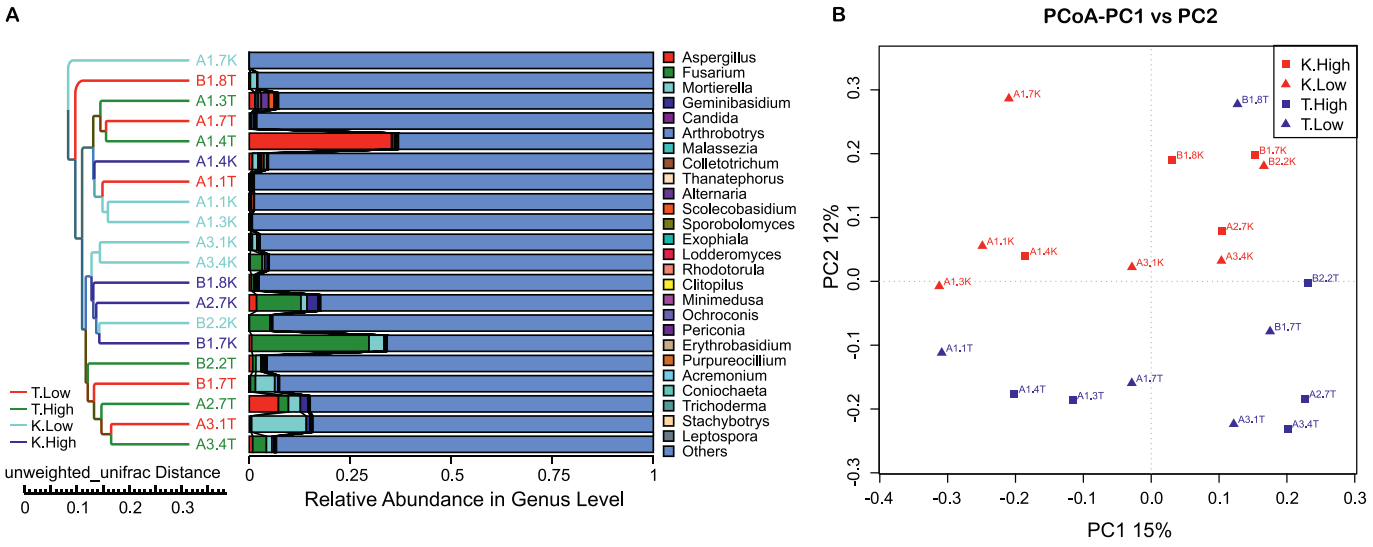

Fig. 2. The composition of fungi populations in sample groups with high and low abundance of A. flavus under different topography. Twenty samples were assigned into 4 groups according to the A. flavus abundance (T. Low and T. High, around-the-pod soil with low or high abundance of A. flavus; K. Low and K. High, on-the-pod samples with low or high abundance of A. flavus). The top 30 abundant species enriched in the 4 groups were illustrated on the right. UPGMA clustering according to the Unweighted Unifrac was shown on the left.

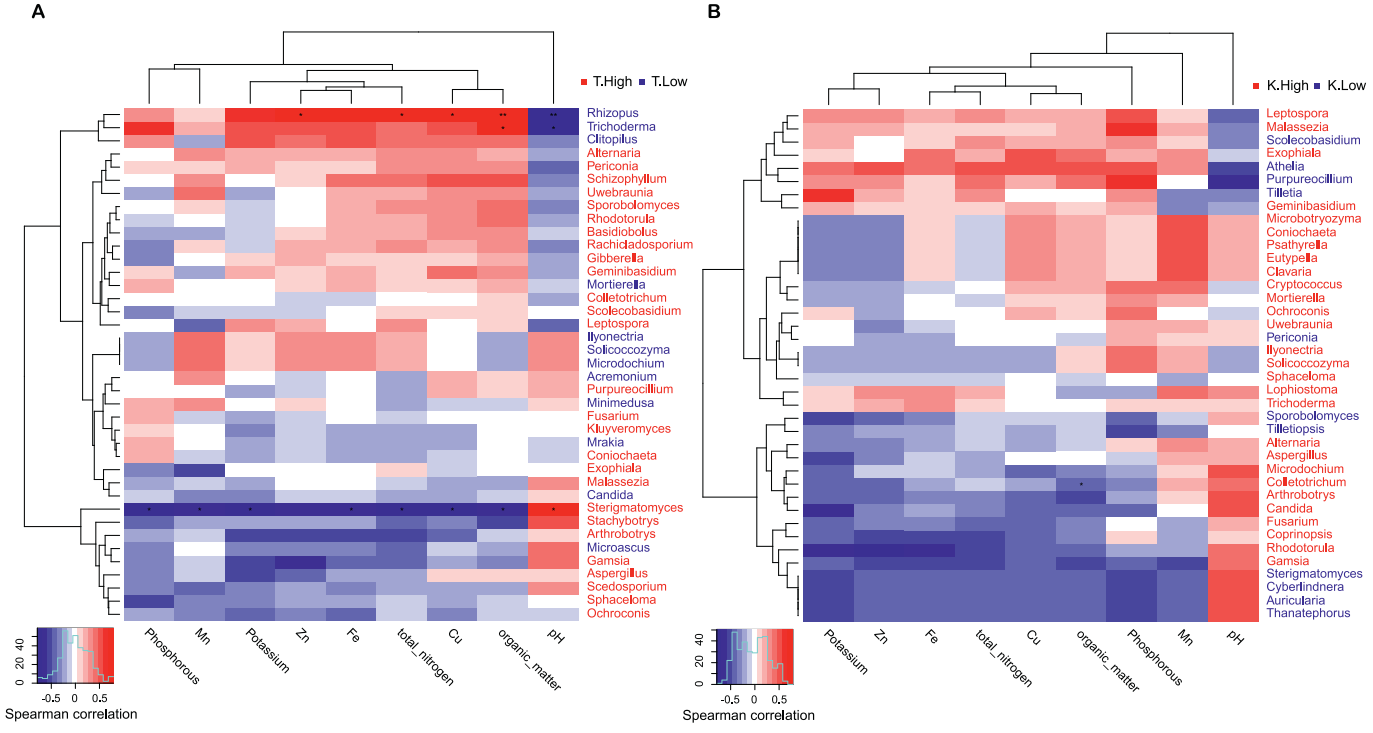

Fig. 3. The correlation analysis between around and on-the-pod fungi species and soil phenotypes under different topography. Correlation between environmental phenotypes and fungi species (A, 10 around-the-pod samples; B, corresponding 10 on-the-pod samples) was analyzed with PERMANOVA (Genus with red labels were significantly enriched in the T. High group while those with green labels were significantly enriched in the T. Low group). The color intensity represents the correlation between species and environmental phenotypes (spearman coefficient). *, $0.01 < p < 0.05$; **, $p < 0.01$. (For interpretation of the references to color in this figure legend, the reader is referred to the web version of this article.)

Principal coordinate analysis (PCoA) based on the Unweight-UniFrac distance showed that the fungal composition from around-the-pod soil samples (red dots) was significantly different from that in on-the-pod samples (blue dots) (Fig. 1C).

In this study, we analyzed the effects of topography and soil physicochemical properties on the microbial population associated with peanuts. Ecological factors were investigated due to their potential effects on microorganism species associated with plant (Tas et al., 2018; Fitzpatrick et al., 2018; Novinscak et al., 2011; Wargo, 2013; Oshiki et al., 2016). Topography can affect the changes in water and nutrients in the soil, which gradually decrease from the downhill position to the uphill position; in particular, the uphill position is prone to

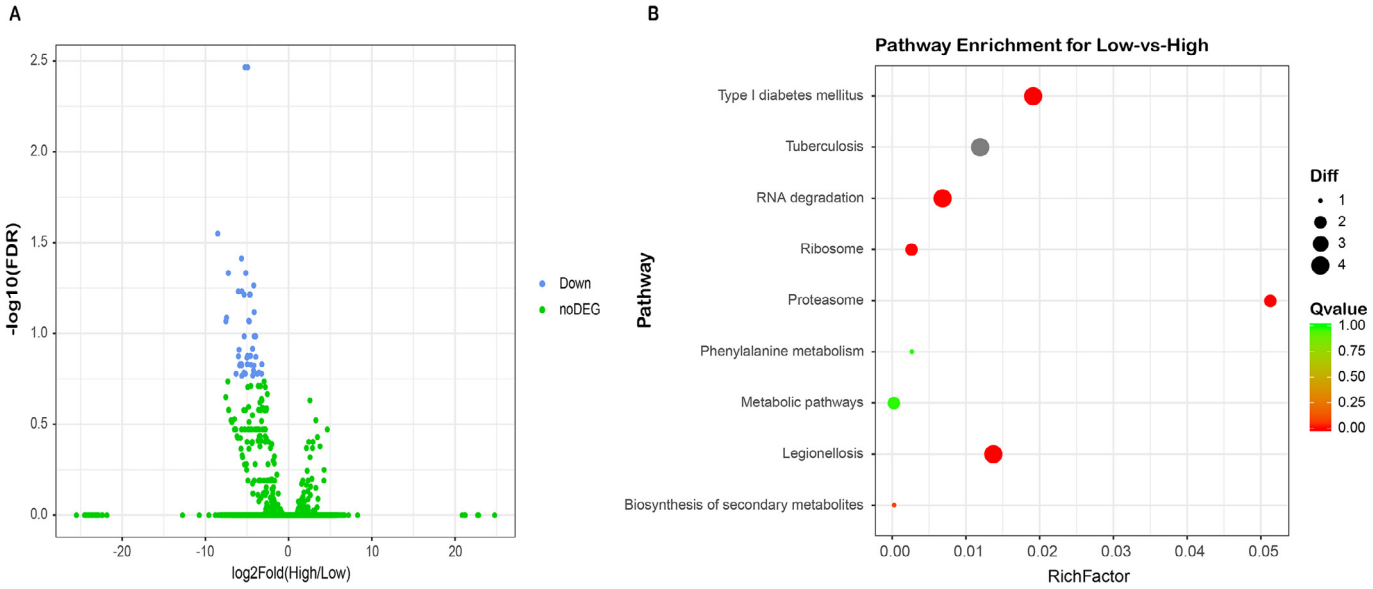

Fig. 4. Metatranscriptomic analysis of gene expression of A. flavus-high and -low groups under different topography. (a) Genes with differential transcriptional levels between A. flavus-high and -low groups were shown in a volcano map. 46 differential expressed genes (DEG) were obtained with DESeq2 analysis ($p < 0.01$). All were enriched in the A.flavus-low group (Blue and green dots represent genes with significant and non-significant expression difference between groups. Down indicated that genes were enriched in A.flavus-low group). (b) The scatter plot of PATHWAY enrichment for differentially expressed genes. The size of the dots corresponds to the number of differentially expressed genes enriched in the pathway; the color of the dots corresponds to the magnitude of Q factor. Rich factor indicates the ratio of the number of differentially expressed genes to the number of all annotated genes in the same pathway. (For interpretation of the references to color in this figure legend, the reader is referred to the web version of this article.)

cause soil drought stress, threaten plant growth and development, and reduce biodiversity (Xiong et al., 2018; Yang et al., 2020; Allen et al., 2010; Alpert et al., 2008; Tas et al., 2018). PCoA analysis based on the unweighted UniFrac distance (Fig. 1C) showed that either around-the-pod or on-the-pod samples from experimental plot A (circle) were evidently distinct from samples collected from experimental plot B (dot). In terms of intra-experimental plot comparisons, all the around-the-pod soil samples at different terrains from plot A showed significant differences in fungal composition, while samples from plot B were less different (uphill position vs. medium position). In terms of intersite comparisons, soil samples at the uphill position and medium position of plot A were also significantly different from their corresponding counterparts of plot B. In both plot A and plot B, fungal composition showed a significant difference between on-the-pod soil samples and around-the-pod samples. Therefore, the composition of fungal communities is affected not only by location but also by terrain. More specifically, Candida grew preferentially in the on-the-pod soil from plot A, while Trichoderma and Microdochium favored on-the-pod soil from plot B. For around-the-pod soil, Geminibasidium, Scolecobasidium, and Alternaria were more enriched at the uphill position of plot A, while Fusarium was the dominant species at the uphill position of plot B. At the level of the medium position, Geminibasidium from plot A, as well as Thanatephorus and Rhodotorula from plot B, were the most enriched populations.

Our research shows that the composition of microbes associated with peanut pods changed with the terrain, while they were also highly consistent according to alpha and beta diversity analysis. This feature implied that plants and symbiotic microorganisms adapted to various environments to maintain healthy growth (Tas et al., 2018).

3.2. Effects of topography on abundance of A. flavus

For ITS sequencing, 10 around-the-pod soil samples were selected based on the abundance of A. flavus (5 lowest vs. 5 highest abundant). Corresponding on-the-pod soil samples were sequenced simultaneously

Table 1
PERMANOVA analysis of OTUs of the 50 samples from 7 groups.

Group1	Group2	F.Model	R^2	P.value	P.adjusted
A1T	A2T	5.05	0.27	0.001	0.002
A1T	A3T	5.02	0.26	0.001	0.002
A1T	B1T	5.28	0.27	0.002	0.003
A2T	A3T	1.87	0.12	0.013	0.015
A1T	A.K	2.56	0.16	0.001	0.002
A1T	B.K	3.65	0.29	0.009	0.011
A2T	B2T	3.63	0.21	0.001	0.002
A2T	A.K	4.91	0.27	0.001	0.002
A3T	A.K	4.46	0.26	0.001	0.002
B1T	B2T	1.46	0.09	0.058	0.058
B1T	B.K	2.11	0.19	0.023	0.025
B2T	B.K	2.99	0.25	0.008	0.011

F. Model, the value of F-test;R^2, means Variation. It is Variance contribution, indicating the explanatory power of different group to differences, that is, the ratio of group variance to total variance. The larger R^2, the higher the explanatory power of groups to differences;p.value, it is Significant when *p*.value <0.05; p.adjusted, the Correction of P value by FDR(false discovery rate).

(Supplementary Table 6). The A. flavus level in both groups of samples positively correlated with the diversity degree of fungal flora (*P*-value = 0.095 for around-the-pod samples, Shannon index low vs. Shannon index high; *P*-value = 0.031 for on-the-pod samples, Shannon index low vs. Shannon index high). Interestingly, fungi living in around-the-pod and on-the-pod soil shared the same degree of diversity and A. flavus abundance (Supplementary Fig. 1), indicating the dynamic enrichment of fungi from soil to pods.

The 20 samples were clustered based on the 30 most abundant fungal genera (UPGMA clustering tree based on unweighted UniFrac distance). As shown in Fig. 2A, the species and annotation ratio varied dramatically. Around-the-pod and on-the-pod samples could not be separated

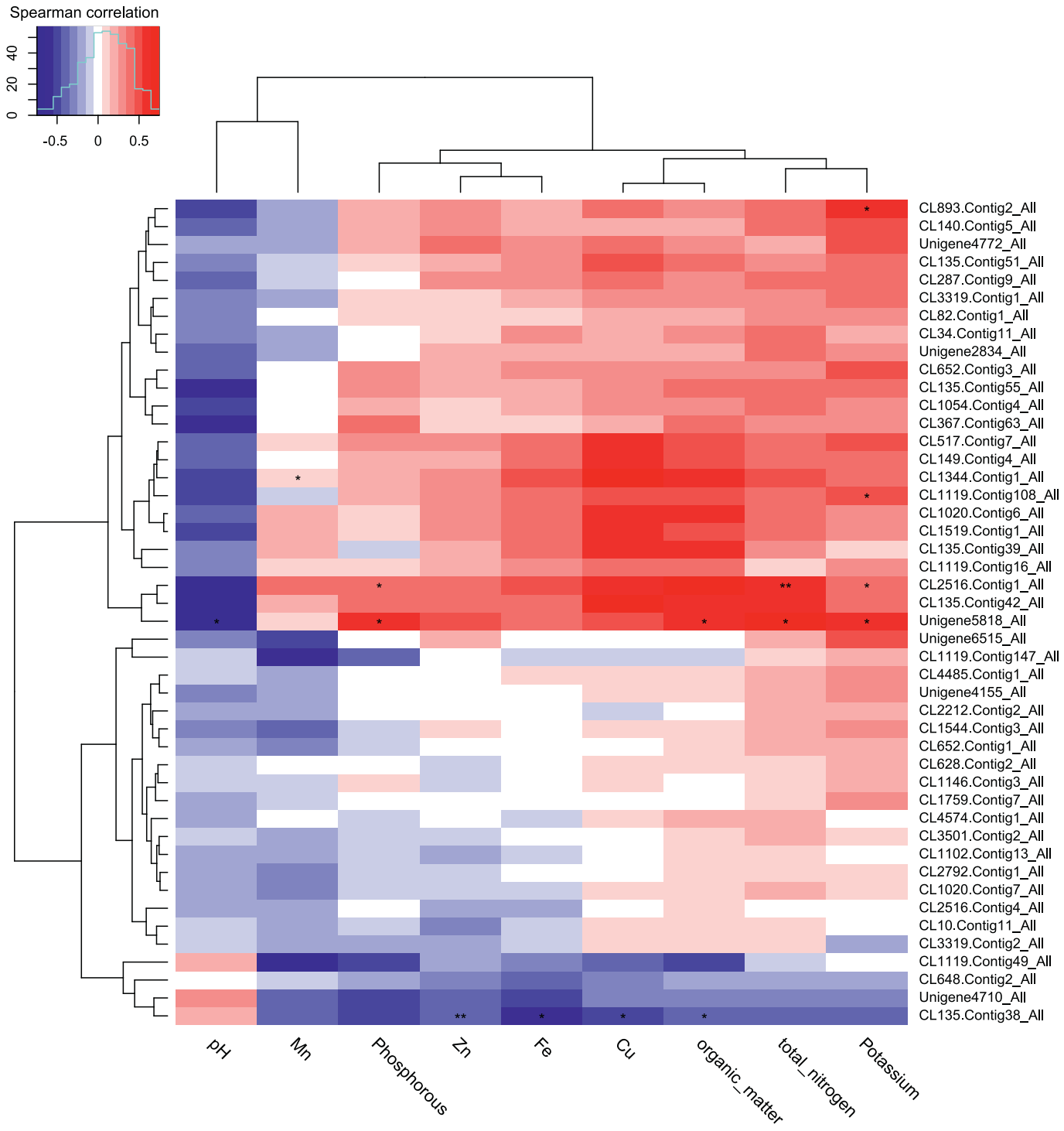

Fig. 5. Correlation analysis between differentially expressed genes and environmental phenotypes (spearman coefficient). PERMANOVA was used to analyze the correlation between environmental phenotypes and differentially expressed genes in Fig. 4. The color intensity represents the correlation strength. *, $0.01 < p < 0.05$; **, $p < 0.01$.

based on the abundance of A. flavus, suggesting the stability of the soil microbial population. PCoA analysis based on unweighted UniFrac distance showed that the samples from plot A at the medium position differed notably from the other samples (Fig. 2B). In addition, around-the-pod samples were clearly distinguished from on-the-pod samples. However, we observed no significance in the comparison between on-the-pod and around-the-pod samples, as well as between groups with low and high abundances of A. flavus and aflatoxin (T. Low vs. T. High: *P*-value = 0.170; K. Low vs. K. High: *P*-value = 0.291, Supplementary Table 7).

In the meantime, we performed a Permanova analysis of species abundance at the genus level and the corresponding phenotypic data of 10 selected around-the-pod soil samples. In the A. flavus-low group, Rhizopus was identified to be positively correlated with total nitrogen, Cu, and organic matter and negatively correlated with pH. In contrast, Trichoderma in the A. flavus-low group showed a positive correlation with

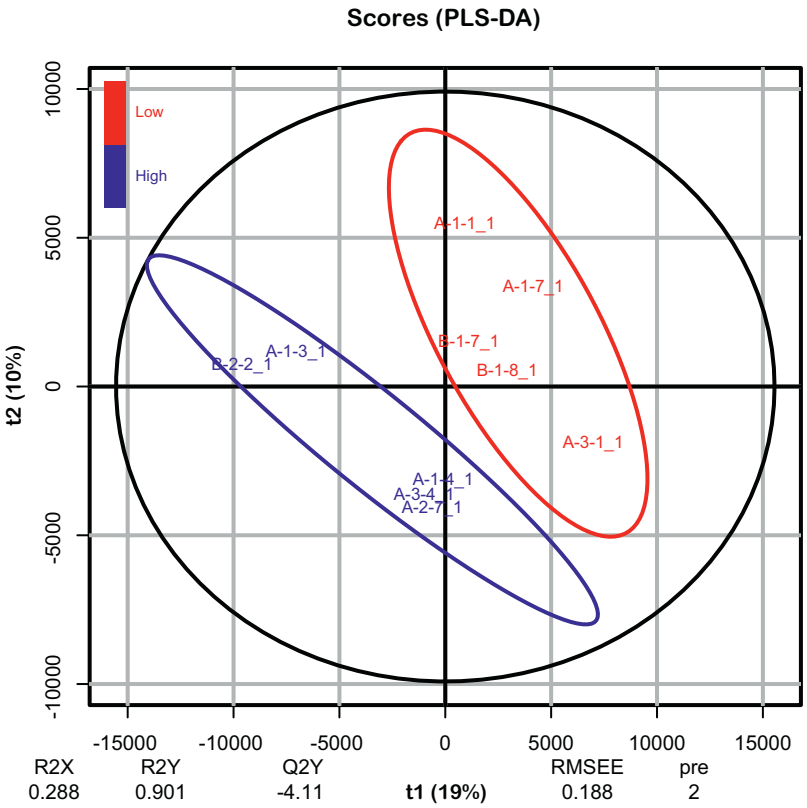

Fig. 6. Properties of around-the-pod fungal metabolomics under different topography. PLS-DA was used to analysis the metabolomics of the around-the-pod samples of A. flavus-high (blue) and -low (red) groups The VIP values of two principal components of PLS-DA (VIP ≥ 0.8), fold change of univariate analyses (Fold Change ≥ 1.2 or ≤ 0.8333), and *p*-value ($p < 0.05$) were combined to screen metabolites with differential expression. (For interpretation of the references to color in this figure legend, the reader is referred to the web version of this article.)

organic matter and a negative correlation with pH. In the A. flavus-high group, Sterigmatomyces was negatively correlated with phosphorous, Mn, potassium, Fe, total nitrogen, Cu, and organic matter and positively correlated with pH (Fig. 3A,B). In conclusion, soil physical and chemical properties have a significant impact on microbial population and can be used to assess microbial diversity under different environmental conditions.

3.3. Effects of topography on the microbial function of peanut

The influence of ecological factors on functions of symbiotic microorganisms was evaluated by metatranscriptome analysis. A total of 112 G high-quality reads were generated with metatranscriptomic sequencing (PE150) of 10 on-the-pod samples (11.2 G per sample). A total of 141,135 genes were annotated with an N50 of 214 bp and an N90 of 150 bp (Supplementary Table 8, Fig. 2A). The RSEM algorithm showed no significant difference between the A. flavus-high and -low groups in terms of transcript expression levels (Supplementary Table 9, Fig. 2B, samples of the A. flavus-low group were clustered together with a p-value = 0.151). There were 46 genes with significantly different expression (DESeq2 analysis), all of which were surprisingly enriched in the A. flavus-low group (Fig. 4A,B, Supplementary Table 10). The results showed that the enrichment of A. flavus in plant roots could significantly affect the microbial population structure and functional expression of peanut pod, regulate the life process of peanut plant, and change the nutrients in peanut pod. Species that can be annotated by these genes were Mycobacterium abscessus, Ralstonia solanacearum, Kutzneria sp.744, Turicella otitidis, and Partitivirus-like 4 (NR as the reference database). Analyses of associated pathways that enriched these genes led to 9 candidates, among which proteasome was the most strongly enriched factor.

Correlations between the 46 differentially expressed genes and the physicochemical properties of soil were further evaluated by Permanova (Fig. 5). CL893 Contig2 All (Mycobacterium abscessus) and CL1119 Contig108_All was positively correlated with potassium and CL1344 Contig1_All was positively correlated with Mn. CL2516 Contig1_All and Unigene5818_All were positively associated with multiple factors, including phosphorous, organic matter, total nitrogen, and potassium, with the latter also associated with organic matter. In contrast, only two genes were negatively correlated with soil physicochemical properties: Unigene5818_All with pH and CL135 Contig38_All with phosphorous, organic matter, total nitrogen, and potassium.

In our experiment, terrain and soil properties could significantly affect the gene expression of microbiome, A. flavus abundance and infection ability to peanuts. Meanwhile, the Permanova correlation analysis revealed that differentially expressed genes were strongly correlated with the soil physicochemical factors. Both domestic and foreign studies have also shown that adverse ecological environments destroy the population structure and function of symbiotic microorganisms of crop rhizospheres and their beneficial symbiosis with plants and reduce the production of resistant substances, such as plant guard elements and fungus-inhibiting proteins, thereby weakening the ability of crop resistance to bacterial pathogens (Ding et al., 2015a,b; Wagner et al., 2016; Muhammad and Wu, 2020). We found that symbiotic fungi associated with peanut pods harvested from different plots shared high consistency in terms of fungal composition and gene function. It is reasonable to speculate that the overall function of the symbiotic microorganisms remains highly conserved, despite the diverse ecological environments. The stability of the plant-related microbial community plays an important role in determining plant adaptability and is affected by many environmental factors (Santhanam et al., 2016; Naylor et al., 2017; Lesk et al., 2016; Jasinska et al., 2015; Liu et al., 2018; Rolli et al., 2015a,b; Chaparro et al., 2014).

3.4. Effects of topography on microbial metabolomics of peanut

When exposed to external stimuli, symbiotic microorganisms respond accordingly as self-defense (Rolli et al., 2015a,b; Chaparro et al., 2014). The study of metabonomics indicated that terrain affected the microorganisms associated with peanut pods to produce a variety of metabolites. The metabolomics of 10 around-the-pod soil samples were analyzed using ChromaTOF software (V 4.3x, LECO) on the mass spec-

Table 2
Metabolites with differential expression levels.

Peak	Low_mean	High_mean	FC	log_2_FC	P-value	FDR	PLS-DA VIP	Diff
Cholesterol-2,2,3,4,4,6-d6	20566.7	61241.9	2.98	1.57	0.01	0.90	0.92	Up
Analyte 167	18613.3	47641.7	2.56	1.36	0.04	0.90	0.80	Up
Analyte 31	94077.7	135450.2	1.44	0.53	0.02	0.90	0.81	Up
Analyte 41	293757.2	370963.7	1.26	0.34	0.04	0.90	0.99	Up
Analyte 24	329213.5	407273.8	1.24	0.31	0.04	0.90	0.99	Up
Ribonicacid, gamma-lactone	227773.8	275149.1	1.21	0.27	0.04	0.90	0.86	Up
gluconic acid 1	150299.0	100400.6	0.67	-0.58	0.04	0.90	1.08	Down
2-Deoxyerythritol	116188.2	64764.32	0.56	-0.84	0.01	0.90	1.25	Down
Analyte 339	42004.9	15448.5	0.37	-1.44	0.01	0.90	0.81	Down

Peak, the identified metabolite; Low and High mean, the average value of metabolites in A. flavus-low and -high groups; FC, fold change of metabolites in A. flavus-high groups versus -low groups; log_2 FC, the log_2 value of FC. *P*-value, the statistical significance; FDR, false discovery rate; PLS-DA VIP, VIP score calculated from PLS-DA; Diff, quantitative expression change of metabolite in A. flavus-high group versus -low group. When multiple peaks correspond to a single compound, only the peak with the highest similarity counts while the others are considered as unknown peaks. Analytes indicates uncharacterized peaks.

trum data after procedures of peak extraction, baseline correction, deconvolution, peak integration, and peak alignment. The LECO-Fiehn Rtx5 database was used to annotate the mass spectrum data. Data processing led to 808 metabolites, among which 164 were recognized in the KEGG database and were potentially involved in 192 metabolism pathways (Fig. 6).

The VIP values of two principal components of PLS-DA (VIP $\geq$ 0.8), fold change of univariate analyses (fold change $\geq$ 1.2 or $\leq$ 0.8333), and *p*-value ($p < 0.05$) were combined to screen metabolites with differential expression (Fig. 6). Eleven of the 808 metabolites that met all three criteria were identified, of which 6 were more abundant in the A. flavus-high group (Cholesterol-2,2,3,4,4,6-d6, Analyte 167, Analyte 31, Analyte 41, Analyte 24, Ribonicacid, gamma-lactone), while the other 3 were more enriched in the A. flavus-low group (Gluconic acid 1, 2-Deoxyerythritol, Analyte 339) (Table 2). In addition, according to the results shown in Supplementary Figure 3, 11 metabolites (i.e., 24,25-dihydrolanosterol, carbobenzyloxy-L-leucine degr1, corticosterone 2, cycloleucine 2, galactose 1, glucose 2, hippuric acid 2, mannitol, mannose 2, trehalose, and xylose 1) were significantly correlated with individual species(Supplementary Fig. 3). The results showed that the differences of metabolites and species in aflatoxin B_1 contaminated plots are closely related to environmental factors.

The correlation between metabolomics and soil physicochemical properties (Cu, Fe, Mn, Zn, pH, organic matter, phosphorous, potassium, and total nitrogen) was examined. Metabolites with a significant correlation with soil properties are listed in Supplementary Table 13. Notably, D-erythro-sphingosine_1, cholesterol-2,2,3,4,4,6-d6, Analyte_47, Analyte_94, Analyte_322, and Analyte_339 were positively correlated with A. flavus. Cholesterol-2,2,3,4,4,6-d6 had no corresponding annotation in the KEGG database, and the last four chemicals were unknown. In contrast, D-erythro-sphingosine_1 was involved in multiple metabolic pathways, such as sphingolipid metabolism, metabolic pathways, sphingolipid signaling pathway, apoptosis, and necroptosis, suggesting that aflatoxin might positively regulate these metabolic pathways which, in turn, reduces peanut quality (Ding et al., 2015a,b) . In addition, our research results showed that different terrains had a significant impact on peanut yield (Supplementary Table 14), and yields of downhill position are higher, we will carry out relevant research in the future (Table 1).

The results of study indicated that there were significant differences in the metabolites between A. flavus-high group and A. flavus-low group, and the specific metabolites could be used as biomarkers to evaluate aflatoxin B_1 contamination in peanuts. Revealing the A. flavus-related symbiotic microorganisms associated with peanut pods, which were also influenced by topographical factors, and a comprehensive understanding of the associated functional genes, as well as metabolites, provide a novel perspective for us to explore a new strategy for A. flavus and aflatoxin B_1 control in peanut planting. Through regulating microorganisms in the peanut rhizosphere and optimizing environmental factors, it becomes plausible to improve peanut yield and quality. Indeed, restraining plant disease has been achieved by rebalancing the homeostasis of rhizosphere microorganisms (Rolli et al., 2015a,b; Marulanda et al., 2009). However, whether this approach will be effective for A. flavus and aflatoxin B_1 prevention is unknown. Therefore, our future will study the microecological management of reducing aflatoxin B_1 contamination in peanuts.

4. Conclusions

Symbiotic microorganisms play an important role in peanut production and are notably affected by ecological environments. In this study, we analyzed the composition and assembly of fungal microflora living in the soil either around the pod or on peanut pods. We elucidated the effects of topography and soil physicochemical properties on the core symbiotic fungi and A. flavus abundance. To the best of our knowledge, this study was the first to examine functional genes and metabolism pathways that integrated the soil physicochemical factors and A. flavus enrichment. We also identified key fungal metabolites that were closely related to A. flavus abundance and analyzed the effects of soil properties on these metabolites. In conclusion, our research showed that topography and soil properties significantly affected fungal floral assembly around and on the pod, enrichment of A. flavus, functional gene expression, and metabolite production. These results may help to characterize fungi associated with disease and could promote healthy peanut production.

Author Contributions

YPY and PWL conceived this project. SYG performed the experiments and analyzed the data. XXD contributed to technical supports. QZ performed the physiochemical characterization of soil and aflatoxin analysis. YPY performed bioinformatics analysis. YPY and QZ wrote the manuscript with the help of all authors. All authors read and approved the final manuscript.

Declaration of competing interest

None.

Acknowledgments

This work was supported by the National Key Research and Development Program of China (2018YFC1602505), National Natural Science Foundation of China (31801665), and The Major Project of Hubei

Provincial Technical Innovation (2018ABA081), and The applied basic research plan of Hebei Province - Key Basic Research Projects (17967502D).

Supplementary materials

Supplementary material associated with this article can be found, in the online version, at doi:10.1016/j.crmicr.2021.100021.

References

Allen, C.D., Macalady, A.K., Chenchouni, H., Bachelet, D., McDowell, N., Vennetier, M., 2010. A global-overview of drought and heat-induced tree mortality reveals emerging climate change risk for forests. Forest Ecol. Manag. 259 (4), 660–684.

Alpert, P., Krichak, S.O., Shafir, H., Haim, D., Osetinsky, I., 2008. Climatic trends to extremes- employing regional modeling and statistical interpretation over the E. Mediterranean. Glob. Planet. Change. 63 (2–3), 163–170.

Archer, P., 2016. Overview of the peanut industry supply chain. In: Stalker, H.T., Wilson, R.F. (Eds.), Peanuts: Genetics, Processing, and Utilization. (Amsterdam:ElsevierInc), pp. 253–266.

Bankole, S., Adebanjo, A., 2004. Mycotoxins in food in West Africa: current situation and possibilities of controlling it. Afr. J. Biotechnol. 2, 254–263.

Barros, G., Torres, A., Palacio, G., Chulze, S., 2003. Aspergillus species from section Flavi isolated from soil at planting and harvest time in peanut-growing regions of Argentina. J. Sci. Food Agric. 83, 1303–1307.

Bokulich, N.A., Subramanian, S., Faith, J.J., Gevers, D., Jeffrey, I., Gordon, J.I., 2013. Quality-filtering vastly improves diversity estimates from Illumina amplicon sequencing. Nat. Methods 10, 57–59.

Buttigieg, P.L., Ramette, A., 2014. A guide to statistical analysis in microbial ecology: a community-focused, living review of multivariate data analyses. FEMS Microbiol. Ecol. 90, 543–550.

Chaparro, J.M., Badri, D.V., Vivanco, J.M., 2014. Rhizosphere microbiome assemblage is affected by plant development. ISME 8, 790–803.

Chen, J., Bittinger, K., Charlson, Emily, S., Hoffmann, C., Lewis, J., Wu, G., 2012. Associating microbiome composition with environmental covariates using generalized UniFrac distances. Bioinformatics 28, 2106–2113.

Chen, Y., Wang, J., Yang, N., Wen, Z., Sun, X., Chai, Y, 2018. Wheat microbiome bacteria can reduce virulence of a plant pathogenic fungus by altering histone acetylation. Nat. Commun. 9, 3429.

Commission of the European Communities (CEC), 2010. Commission regulation (EU) No 165/2010 of 26 February 2010 amending Regulation (EC) No 1881/2006 setting maximum levels for certain contaminants in food stuffs as regards aflatoxins. Off. J. Eur. Union. 50, 8–12.

Dan, N., Stephanie, D.G., Elizabeth, P., Devin, C.D., 2017. Drought and host selection influence bacterial community dynamics in the grass root microbiome. ISME J. 11, 2691–2704.

Devin, C.D., Damaris, D., Citlali, F.G., Stephen, G., 2016. Plant compartment and biogeography affect microbiome composition in cultivated and native Agave species. New Phytol. 209, 798–811.

Ding, N., Xing, F., Liu, X., Selvaraj, J.N., Wang, L., Zhao, Y., 2015a. Variation in fungal microbiome (mycobiome) and aflatoxin in stored in-shell peanuts at four different areas of China. Front. Microbiol. 6, 1055.

Ding, X.X., Wu, L.X., Li, P.W., 2015b. Risk assessment on dietary exposure to aflatoxin B1 in post-harvest peanuts in the Yangtze River ecological region. Toxins 7, 4157–4174.

Dong, Y.J., Chen, W.F., Zhuge, Y.P., Song, Y.L., Hu, G.Q., Wan, Y.S., Liu, F.Z., Li, X, 2018. Effect of application of exogenous nitric oxide at different critical growth stages in alleviating Fe deficiency chlorosis of peanut growing in calcareous soil. J. Plant Nutr. 47, 867–887.

Edgar, R.C., 2018. Taxonomy annotation and guide tree errors in 16S rRNA databases. Peer J. 6, 5030.

Fitzpatrick, C.R., Copeland, J., Wang, P.W., Guttman, D.S., Kotanen, P.M., Johnson, M.T.J., 2018. Assembly and ecological function of the root microbiome across angiosperm plant species. Proc. Natl. Acad. Sci. USA 115, 1157–1165.

Giorni, P., Magan, N., Battilani, P., 2009. Environmental factors modify carbon nutritional patterns and niche overlap between Aspergillus flavus and Fusarium verticillioides strains from maize. Int. J. Food. Microbiol. 130, 213–218.

Han, L.Z., Liu, C., Zhou, J., 2019. Effects of inoculation with growth-promoting bacteria on peanut rhizosphere soil microorganism and nutrient elements. In: Genom. Appl. Biol., 38, pp. 3065–3073.

Jasinska, E.J., Goss, G.G., Gillis, P.L., Van Der Kraak, G.J., Matsumoto, J., Machado, A.A.D., Giacomin, M., Moon, T.W., Massarsky, A., Gagne, F., Servos, M.R., Wilson, J., Sultana, T., Metcalfe, C.D., 2015. Assessment of biomarkers for contaminants of emerging concern on aquatic organisms down stream of a municipal wastewater discharge. Sci. Total Environ. 530, 140–153.

Koljalg, U., Nilsson, R.H., Abarenkov, K., Tedersoo, L., Taylor, A.F.S., Bahram, M., 2013. Towards a unified paradigm for sequence-based identification of fungi. Mol. Ecol. 22, 5271–5277.

Lesk, C., Rowhani, P., Ramankutty, N., 2016. Influence of extreme weather disasters on global crop production. Nature 529, 84–87.

Liu, J., Chen, X., Shu, H.Y., Lin, X.R., Zhou, Q.X., Bramryd, T., Shu, W.S., Huang, L.N., 2018. Microbial community structure and function in sediments from e-waste contaminated rivers at Guiyu area of China. Environ. Pollut. 235, 171–179.

Love, M.I., Huber, W., Anders, S., 2014. Moderated estimation of fold change and dispersion for RNA-seq data with DESeq2. Genome Biol. 15, 550.

Marulanda, A, Barea, J-M, Azcón, R, 2009. Stimulation of plant growth and drought tolerance by native microorganisms (AM fungi and bacteria) from dry environments: mechanisms related to bacterial effectiveness. Plant Growth Regul. 28, 115–124.

Muhammad, N., Wu, J.H., 2020. Stability of microbial functionality in anammox sludge adaptation to various salt concentrations and different salt-adding steps. Environ. Pollut. 264, 1–4.

Nataraj, K.C., Babu, M.V., Narayanaswamy, G., Bhargavi, K., Reddy, B.S., Rao, C.S., 2016. Nutrient management strategies in groundnut-based crop production systems in dryland regions of southern Andhra Pradesh. Indian J. Fertil. 16 (10), 58–75.

Naylor, D., Degraaf, S., Purdom, E., 2017. Drought and host selection influence bacterial community dynamics in the grass root microbiome. ISME 11, 2691–2704.

Novinscak, A., Filion, M., 2011. Effect of soil clay content on RNA isolation and on detection and quantification of bacterial gene transcripts in soil by quantitative reverse transcription-PCR. Appl. Environ. Microbiol. 77, 6249–6252.

Oshiki, M., Satoh, H., Okabe, S., 2016. Ecology and physiology of anaerobic ammonium oxidizing bacteria. Environ. Microbiol. 18, 2784–2796.

Passone, M.A., Rosso, L.C., Ciancio, A., Etcheverry, M., 2010. Detection and quantification of Aspergillus section Flavi spp. in stored peanuts by real-time PCR of nor-1 gene, and effects of storage conditions on aflatoxin production. Int. J. Food Microbiol. 138, 276–281.

Quast, C., Pruesse, E., Yilmaz, P., Gerken, J., Schweer, T., Yarza, P., 2013. The SILVA ribosomal RNA gene database project: improved data processing and web- based tools. Nucleic Acids Res. 41, 590–596.

Rolli, E., Azcón, R., Vigani, G., 2015a. Improved plant resistance to drought is promoted by the root associated microbiome as a water stress-dependent trait. Environ. Microbiol. 17, 316–331.

Rolli, E., Marasco, R., Vigani, G., 2015b. Improved plant resistance to drought is promoted by the root associated microbiome as a water stress-dependent trait. Environ. Microbiol. 17, 316–331.

Santhanam, R., Rowhani, P., Lebeis, S.L., 2016. Specificity of root microbiomes in native–grown Nicotiana attenuata and plant responses to UVB increase Deinococcus colonization. Mol. Ecol. 26, 2543–2562.

Santos, C.C.M., Lopes, M.R.V., Kosseki, S.Y., 2001. Ocorrêcia de aflatoxinas em amendoim e produtos de amendoim comercializados naregiã de São José de Rio Preto/SP. Rev. Inst. Adolfo Lutz 60, 153–157.

Santos, R.C.D., 2000. Nova cultivar de amendoim para as condiçoes do nordeste brasileiro. Pesq. Agrop. Bras. 35, 665–670.

Subhashini, D.V., 2016. Improved growth and nutrient uptake in peanut inoculated with Glomus intraradices. Ann. Plant Prot. Sci. 24, 145–147.

Taş, N., Prestat, E., Wang, S., Wu, Y.X., Ulrich, C., Kneafsey, T., 2018. Land scape topography structures the soil microbiome in arctic polygonal tundra. Nat. Commun. 9, 777.

Wagner, M.R., Paredes, S.H., Degraaf, S., 2016. Host genotype and age shape the leaf and root microbiomes of a wild perennial plant. Nat. Commun. 7, 12151.

Wargo, M.J., 2013. Homeostasis and catabolism of choline and glycine betaine: lessons from Pseudomonas aeruginosa. Appl. Environ. Microbiol. 79, 2112–2120.

Williams, J.H., 2004. Human aflatoxicosis in developing countries: a review of toxicology, exposure, potential health consequences, and interventions. Am. J. Clin. Nutr. 80, 1106–1122.

Wu, L.X., Ding, X.X., Li, P.W., 2016. Aflatoxin contamination of peanuts at harvest in China from 2010 to 2013 and its relationship with climatic conditions. Food Control 60, 117–123.

Xia, Z., Wang, Q., She, Z., Gao, M., Zhao, Y., Guo, L., Jin, C., 2019. Nitrogen removal pathway and dynamics of microbial community with the increase of salinity in simultaneous nitrification and denitrification process. Sci. Total Environ. 697, 134047.

Xiong, K., Yin, C., Ji, H.B., 2018. Soil erosion and chemical weathering in a region with typical karst topography. Environ. Earth Sci. 77 (13), 215.

Yang, L.S., Feng, Q., Yin, Z.L., Deo, R.C., Wen, X.H., Si, J.H., Liu, W., 2020. Regional hydrology heterogeneity and the response to climate and land surface changes in arid alpine basin, northwest China. Catena 13. doi:10.1016/j.catena.2019.104345.

Zhang, D.H., Li, P.W., Zhang, Q., 2015. Ultrasensitive enanogold probe-based Immunochromatographic assay for simultaneous detection of total aflatoxins in peanuts. Biosens. Bioelectr. 26 (6), 2877–2882.

Zhang, M., Wang, L., Cheng, X., Wang, Y., Zhang, J., 2019. Application of external heating digestion-air cooled tube reflow in the determination of soil organic matter content. Contemp. Chem. Ind. 48, 2129–2131.

Zhao, Y.J., Liu, J.L., Zhang, Y.B., Liu, S., Sun, H.J., 2019. The response of spring peanut to nitrogen, phosphorus and potassium in Eastern Hebei Province. Acta Agric. Boreali-Sin. 34, 192–198.